



Published in final edited form as:

Hear Res. 2008 January ; 235(1-2): 114–124. doi:10.1016/j.heares.2007.10.010.

A systemic gentamicin pathway across the stria vascularis

Chun Fu Dai^{1,2} and Peter S Steyger^{1,*}

1 Oregon Hearing Research Center, Oregon Health Sciences University, 3181 SW Sam Jackson Park Road, Portland, Oregon, 97239

2 Dept. of Otolaryngology, Eye Ear Nose and Throat Hospital, Fudan University, Shanghai, 200031, P.R. China

Abstract

The mechanism(s) by which systemically-administered aminoglycosides enter the cochlea remain poorly understood. To elucidate which mechanisms may be involved, we co-administered different molar ratios of gentamicin and fluorescent gentamicin (GTTR) to mice in three different regimens: (1) gentamicin (150, 300 or 600 mg/kg) containing a constant 300:1 molar ratio of gentamicin:GTTR; (2): 300 mg/kg gentamicin containing a variable molar ratio of gentamicin:GTTR (150:1–600:1), or (3): an increasing dose of gentamicin (150–900 mg/kg), each dose containing 1.7 mg/kg GTTR. Three hours later, cochleae were fixed and examined by confocal microscopy.

First, increasing doses of a constant molar ratio of gentamicin:GTTR, resulted in increasing intensities of GTTR fluorescence in hair cells and strial tissues. Second, a fixed gentamicin dose with increasing molar dilution of GTTR led to decreasing GTTR fluorescence in hair cells and strial tissues. Third, a fixed GTTR dose with increasing molar dilution by gentamicin led to decreased GTTR uptake in hair cells and marginal cells, but not intra-strial tissues and capillaries. Thus, only hair cell and marginal cell uptake of GTTR is competitively inhibited by gentamicin, suggesting that a regulatable barrier for gentamicin entry into endolymph exists at the interface between marginal cells, the intra-strial space and intermediate cells.

Keywords

gentamicin; blood-labyrinth barrier; ototoxicity; aminoglycosides; cochlea; hair cells; stria vascularis

INTRODUCTION

The nephrotoxicity and ototoxicity of aminoglycosides are well-known, but the mechanisms by which aminoglycosides enter the cochlea in vivo still remains poorly understood. Pharmacokinetic studies show that aminoglycoside concentrations in endolymph follow the rise, but not the subsequent fall that is observed in serum and perilymphatic concentrations of these ototoxic drugs following systemic administration. Thus, clearance of aminoglycosides from endolymph is very slow, and cochlear tissues retain aminoglycosides far longer than

*Correspondence should be addressed to: P.S. Steyger, Ph.D., Oregon Hearing Research Center, Oregon Health & Science University, 3181 Sam Jackson Park Road, Portland, OR 97239 USA., FAX: (+1) 503-494-5656, Voice: (+1) 503-494-1062, E-mail: E-mail: steygerp@ohsu.edu.

Publisher's Disclaimer: This is a PDF file of an unedited manuscript that has been accepted for publication. As a service to our customers we are providing this early version of the manuscript. The manuscript will undergo copyediting, typesetting, and review of the resulting proof before it is published in its final citable form. Please note that during the production process errors may be discovered which could affect the content, and all legal disclaimers that apply to the journal pertain.

serum (Dulon et al., 1986; Dulon et al., 1993; Hiel et al., 1992; Tran Ba Huy et al., 1986; Tran Ba Huy et al., 1983b).

Neonatal murine cochlear hair cells rapidly take up systemically-administered aminoglycosides, including gentamicin-conjugated Texas Red (GTTR), and also AM1–43 (Bernard, 1981; Dai et al., 2006; Henry et al., 1981; Lenoir et al., 1983; Meyers et al., 2003; Pujol, 1986), prior to the development of a functional blood-labyrinth barrier (BLB) in the stria vascularis and endocochlear potential that occurs between post-natal days 12–15 (Ehret, 1976; Shnerson and Pujol, 1981). However, after maturation of the BLB, murine hair cells no longer take up AM1–43 (Meyers et al., 2003). In contrast, GTTR is taken up by hair cells in adult murine cochleae over time (Dai et al., 2006). Thus GTTR, unlike AM1–43, is able to cross the functionally mature BLB, like other aminoglycosides.

Co-administration of GTTR and ethacrynic acid (a loop diuretic that disrupts the stria BLB), results in enhanced uptake of GTTR by both stria tissues and hair cells (Dai et al., 2006), confirming previous reports that ethacrynic acid synergistically enhances aminoglycoside uptake and ototoxicity (Brummett, 1981; Hayashida et al., 1989; Mathog and Capps, 1977; Rybak, 1982; Tran Ba Huy et al., 1983a; Yamane et al., 1988). Thus, the stria BLB is an important barrier for preventing the entry of aminoglycosides into the cochlea and subsequent ototoxicity.

How might GTTR, and hence aminoglycosides cross the BLB? There are several possible mechanisms. Firstly, extravasation (paracellular transport between endothelial cells) from cochlear arteries, which can be enhanced by capsaicin, electrical stimulation of the trigeminal ganglion, and serotonin (Koo and Balaban, 2006; Vass et al., 2001). Secondly, passage through the damaged membranes of necrotic BLB cells, perhaps induced by drug toxicity, thus increasing barrier leakiness. Thirdly, transcytosis across stria endothelial cells comprising the stria BLB (Sakagami et al., 1982), and/or fourthly, a cell-regulated, transcellular transport across the BLB reminiscent of non-endocytotic uptake in vitro (Myrdal et al., 2005). In that study, we demonstrated that cytoplasmic uptake of GTTR can be competitively inhibited by increasing concentrations of native unconjugated gentamicin in vitro. Therefore, to potentially determine which of these possible mechanisms GTTR uses to enter the cochlea in vivo, we subcutaneously injected various molar ratios of gentamicin:GTTR and examined cochlear and renal tissues. The results show that only hair cell and marginal cell uptake of GTTR is competitively inhibited by gentamicin, but not in deeper lying stria tissues or capillaries. The data suggest that a regulatable barrier for gentamicin entry into endolymph exists at the interface between marginal cells, the intra-stria space and intermediate cells.

METHODS

Gentamicin sulfate (Sigma; 50 mg/mL in K₂CO₃, pH 9) and succinimidyl esters of Texas Red (Invitrogen, CA; 2mg/mL in dimethyl formamide) were agitated together for several days at 4°C to produce a gentamicin-Texas Red conjugate (GTTR). Typically, 4.4 ml of 50 mg/ml (final volume) gentamicin (GT; M.W. = 449–477) was mixed with 0.6 mL of 2 mg/mL Texas Red esters (M.W. = 817) to produce an approximately 300:1 molar ratio of GT:GTTR. A high ratio of free GT to Texas Red esters ensures that only one Texas Red molecule is conjugated to any individual GT conjugate (Sandoval et al., 1998).

Juvenile (21–28 day old) C56/BL6 mice received one subcutaneous injection according to the following protocol (summarized in Table 1): **Regimen 1:** 150, 300 or 600 mg/kg GT containing a constant 300:1 molar ratio of GT:GTTR. **Regimen 2:** 300 mg/kg GT containing either 150:1, 300:1 or 600:1 molar ratio of GT:GTTR. **Regimen 3:** 1.7 mg/kg GTTR regardless of the GT dose given (150, 300, 600, and 900 mg/kg). Control mice received equivalent doses of

hydrolyzed Texas Red (hTR), with various doses of unconjugated GT. At least three animals were used and examined for each dose in each regimen.

At 3 hours post-injection, animals were anesthetized prior to excision of kidneys and cochleae for fixation in 4% formaldehyde overnight. Kidneys were then vibrotome-sectioned at 10 μ m. After washing in PBS, all specimens were permeabilized using ice-cold acetone, and labeled with Alexa-488-conjugated phalloidin to localize filamentous actin. Specimens were whole-mounted in VectaShield (Vector Labs, CA) and observed using a Bio-Rad MRC 1024 ES laser scanning confocal system attached to a Nikon Eclipse TE300 inverted microscope. Alexa-488 and Texas Red images were collected sequentially using 1024 \times 1024 pixel box size using a 60 \times lens (n.a. 1.4) with an xy resolution = 230 nm and xz resolution = 440 nm. For each dosing regimen, all specimens were imaged at the same laser intensity and gain settings, including control tissues. Representative images from each dose regimen were identically prepared for publication using Adobe PhotoShop.

For image analysis, optical sections from each experimental set were identified, and regions of interest (OHCs, marginal cells [minus nuclei], tissues between strial capillaries, and strial capillaries) were isolated for pixel intensity determination (ImageJ, NIH). To normalize data between experimental sets, the mean intensity was ratioed against the standard (300:1 GT:GTTR, 300 mg/kg) and plotted. Student's t-test was used to determine any significant difference between groups in the same regimen.

RESULTS

Distribution of fluorescence and experimental controls

Three hours after subcutaneous injection of GTTR, the distribution of GTTR fluorescence in cochlear hair cells, strial and kidney tissues were similar to those previously described (Dai et al., 2006). In the stria vascularis, GTTR fluorescence was most prominent in the tissues associated with the strial capillaries, with less intense, diffuse fluorescence in the tissues between the capillaries (Fig. 1A). Intense fluorescent puncta were readily visible in the immediate vicinity of strial capillaries. In the spiral ligament, little GTTR fluorescence was observed, with fewer fluorescent puncta associated with spiral ligament capillaries (compared to strial capillaries, data not shown). GTTR fluorescence was also observed in marginal cells, delineating the nuclei (Fig. 1D). Mice injected with hTR (equivalent to the highest doses of GTTR), together with unconjugated gentamicin, display negligible fluorescence in strial tissues (Fig. 1B,E). These control images were acquired using the same laser intensity and confocal settings as tissues dosed with GT:GTTR. The focal planes identifying the stria vascularis for control images were confirmed by phalloidin labeling in the green channel, particularly the actiniferous junctional complexes of marginal cells (Fig. 1C,F).

In the organ of Corti, GTTR fluorescence was present in outer hair cells (OHCs) inner hair cells (IHCs) and pillar cells, with less intense fluorescence in the Hensen's cells (Fig. 1G). Puncta of autofluorescence at emission wavelengths similar to Texas Red was observed in the supporting cells surrounding the IHCs, as previously described (Dai et al., 2006), in both GTTR- and hTR-treated tissues (Fig. 1G,H,J,K). This autofluorescence is discounted in all subsequent descriptions. Negligible hTR fluorescence was observed in the organ of Corti (Fig. 1H). The focal planes identifying the organ of Corti for control images were confirmed by phalloidin labeling (Fig. 1I,L). To determine if potentially acute aminoglycoside toxicity enhanced cochlear uptake of hTR, high doses of GT (900 mg/kg) were administered with hTR, yet negligible hTR fluorescence was observed in the organ of Corti (Fig 1K) and strial tissues (data not shown). When equivalent doses of GTTR were administered with the same high dose of GT, GTTR fluorescence could be observed in the organ of Corti (Fig. 1J; see also Regimen

3 and Fig. 4 below). All descriptions of GTTR uptake within the cochlea in this study are from the mid-basal region.

In the kidney, GTTR fluorescence was concentrated in the proximal tubules identified by their actiniferous brush border labeled by phalloidin (as in Fig 1O). Proximal tubule cells contained both punctate and diffuse (cytoplasmic) GTTR fluorescence (Fig. 1M). Much less intense diffuse cytoplasmic GTTR fluorescence was also observed in distal tubule cells (Fig. 1M). Subcutaneous injection of hTR (with GT) revealed negligible hTR fluorescence in kidney tissues (Fig. 1N). The focal planes identifying proximal tubules, and their actiniferous brush border, were confirmed by phalloidin labeling (Fig. 1O).

Regimen 1: Constant GT:GTTR ratio

Mice received a single injection of 150, 300 or 600 mg/kg GT, each dose containing a constant 300:1 molar ratio of GT:GTTR, three hours before cochlear fixation (Table 1). With increasing total dose of GT, increased intensities of GTTR fluorescence are observed in hair cells (Fig. 2A–C), marginal cells (Fig. 2D–F) and intra-strial tissues (putatively the intermediate cells and intra-strial space) and capillaries (Fig. 2G–I). GTTR fluorescence was typically diffuse within the soma of IHCs and OHCs (Fig. 2A–C), and stereocilia were readily observed at higher doses (600 mg/ml, 300:1 GT:GTTR, Fig. 2C). Less GTTR fluorescence was observed in the majority of surrounding supporting cells (Deiters' cells, Hensen's cells) although pillar cells appeared to display almost equivalent intensities of GTTR fluorescence.

In the stria vascularis, marginal cells displayed increasing intensities of GTTR fluorescence with increasing dose. Within the stria vascularis, the tissues immediately surrounding strial capillaries also displayed increased intensities of GTTR fluorescence at higher doses. Also at higher doses, the tissues between the capillaries (intra-strial tissues) exhibited diffuse fluorescence, although it could not be determined whether this was somatic or extracellular fluorescence (Fig. 2I). At high doses, marginal cells and intra-strial tissues displayed diffuse fluorescence, with few fluorescent puncta (Fig. 2D–I). In contrast, the strial capillaries and the tissues immediately surrounding them displayed abundant fluorescent puncta, reminiscent of endosomes (Fig. 2H,I).

Regimen 2: Constant GT dose, varying GTTR dose

In contrast to Regimen 1, mice received a constant dose of GT (300 mg/kg), each dose containing either 150:1, 300:1 or 600:1 molar ratio of GT:GTTR. Thus, each animal received the same GT dose, with a variable GTTR dose. With increasing molar dilution of GTTR, decreasing intensities of GTTR fluorescence occurred in hair cells (Fig. 3A–C), marginal cells (Fig. 3D–F) and intra-strial tissues and capillaries (Fig. 3G–H). At low molar dilution of GTTR (150:1 GT:GTTR), marginal cells and intra-strial tissues displayed diffuse fluorescence, with few fluorescent puncta (Fig. 3D–I), compared to the strial capillaries (and immediately adjacent tissues) that had many fluorescent puncta (Fig. 3G,H).

Regimen 3: Variable GT dose, constant GTTR dose

In contrast to the previous dosing regimens, mice received a constant dose of GTTR (equivalent to 1.7 mg/kg) regardless of the total GT dose given (150, 300, 600, or 900 mg/kg). With increasing GT dose, decreasing intensities of GTTR fluorescence were generally observed in hair cells (Fig. 4A–D), marginal cells (Fig. 4E–H), but not in intra-strial tissues or capillaries (Fig. 4I–L). At low GT doses (150 mg/kg; 150:1 GT:GTTR), GTTR fluorescence occurred in hair cells, and surrounding supporting cells, marginal cells, with less intense fluorescence in the tissues between the strial capillaries. At higher molar dilutions (e.g., 300 mg/kg, 300:1 GT:GTTR and 600 mg/kg, 600:1 GT:GTTR), less intense GTTR fluorescence occurred in OHCs and marginal cells tissues (Fig. 4B,C,F,G), but not in intra-strial tissues (Fig. 4J,K). In

the capillaries, the fluorescence intensity appeared consistent between different GT doses, reflecting the constant GTTR dose administered. At very high molar dilutions (e.g., 900 mg/kg, 900:1 GT:GTTR), GTTR fluorescence intensity appeared slightly more intense in hair cells and marginal cells (Fig. 4D,H) than at the 600:1 GT:GTTR dose.

To confirm the potential inhibition of GTTR uptake in OHCs and marginal cells by unconjugated gentamicin, we vibrotome-sectioned kidney tissues from the same animals (Fig. 5A–C). At higher molar dilutions of a constant GTTR dose, decreased cytoplasmic uptake of GTTR occurred in proximal tubule cells occurred, and especially at the 900:1 molar dilution of GT:GTTR (Fig. 5C). In addition, high doses of GT did not appear to reduce the density of fluorescent puncta in proximal tubule cells (Fig. 5C).

Figure 5D shows the intensity of GTTR fluorescence in the cytoplasm of OHCs, marginal cells and proximal tubule cells. GTTR intensity is greatest at the lowest molar ratio of GT:GTTR (i.e., at 150 mg/kg GT). Increasing the GT dose generally decreases GTTR intensity (i.e., increased molar dilution of a constant dose of GTTR), particularly in kidney proximal tubule cells. However, the intensity of cytoplasmic GTTR fluorescence in OHC and marginal cells at the highest dose of 900 mg/kg GT was significantly increased from the 600 mg/kg dose ($p < 0.05$), and was not significantly different from the 300mg/kg dose ($p > 0.05$). In contrast, GTTR fluorescence in strial capillaries and the intra-strial tissues was not significantly different ($p > 0.05$) from other doses (data not shown).

DISCUSSION

Although guinea pigs have been the preferred rodent model for aminoglycoside ototoxicity that occur in humans, a murine model for ototoxicity has been developed to exploit the rapidly expanding array of genetically-engineered mice with which to investigate the mechanisms of drug cytotoxicity in the inner ear (Wu et al., 2002; Wu et al., 2001). Recently, we reported that adult mice had substantially reduced hair cell uptake of GTTR compared to neonatal mice, or guinea pigs, receiving equivalent doses (Dai et al., 2006; Wu et al., 2002). The reduced uptake of GTTR in adult murine hair cells corresponds with the need for adult mice to receive greater aminoglycoside doses regimens to induce a similar degree of auditory dysfunction and anatomical damage observed in guinea pigs and humans (Wu et al., 2001). However, murine cochlear hair cells are equally sensitive to acute aminoglycoside administration *in vitro* as guinea pig hair cells (Dehne et al., 2002; Dulon et al., 1989; Gale et al., 2001; Richardson and Russell, 1991), suggesting that the murine blood-labyrinth barrier (BLB) may be more effective in excluding systemically-administered aminoglycosides from the cochlear fluids (assuming that serum concentrations of aminoglycosides are consistent across species). This efficacious cochlear barrier to aminoglycoside uptake in mice allowed us to test the hypothesis that aminoglycoside transport across the strial BLB is regulatable, with fewer confounding transport routes, such as paracellular transport, that may exist in other mammals.

Aminoglycosides may enter cochlear hair cells (i) across the basolateral plasma membrane of hair cells from cortilymph (similar to perilymph) within the organ of Corti, or (ii) across the apical membrane of hair cells from the endolymph. The evidence that aminoglycosides enter hair cells from endolymph and induce cytotoxicity *in vivo* is based on *in vitro* studies demonstrating that the mechano-electrical transduction channel is aminoglycoside-permissive (Gale et al., 2001; Marcotti et al., 2005), and the presence of aminoglycoside-laden endosomes at the apex of hair cells *in vivo* (Aran et al., 1993; Hashino and Shero, 1995). In addition, aminoglycosides, GTTR, and fluorophores cross the apical membrane of hair cells in zebrafish lateral line neuromasts (Harris et al., 2003; Owens et al., 2007; Ton and Parng, 2005). Although, this endolymphatic route has yet to be verified for mammals *in vivo*, perfusion of the scala tympani with artificial perilymph containing aminoglycosides did not rapidly interfere with

hair cell transduction and afferent neural activity (Aran et al., 1999). In toto, these data suggest that aminoglycoside uptake by hair cells (and subsequent toxicity) occurs primarily via the endolymph.

Junctional complexes between adjacent epithelial cells, including stria marginal cells, lining the scala media enclose the endolymphatic scala media to form an impermeable paracellular barrier between endolymph and perilymph. The BLB is also composed of junctional complexes between adjacent endothelial cells in cochlear capillaries, particularly in the lateral wall (Juhn et al., 2001; Sakagami et al., 1982). Thus, the composite BLB between serum and cochlear fluids appears likely to be an intrinsic factor that determines the degree of aminoglycoside uptake and subsequent toxicity within the cochlea. If aminoglycosides enter hair cells from endolymph, how could they enter endolymph? One potential route is to cross the BLB within the highly-vascularized stria vascularis (Steyger, 2005). Therefore, we used native, unconjugated gentamicin to potentially modulate GTTR entry into the cochlea, and attempt to determine which transport routes may be involved in aminoglycoside transport across the BLB.

Regimen 1: Constant GT:GTTR ratio

In this study, the distribution of GTTR in hair cells, stria capillaries and kidney tissues is similar to that reported previously, using a 300:1 molar ratio (Dai et al., 2006). In addition, we also observed GTTR fluorescence in marginal cells, in the intra-stria tissues (putatively the intermediate cells and intra-stria space), and in distal tubule cells of the kidney. The latter observations corroborate recent descriptions of aminoglycoside uptake by distal tubule cells in vitro (Myrdal et al., 2005). Significantly, as the total dose of GTTR increased, or the molar dilution of GTTR by GT was reduced, greater GTTR fluorescence was observed in hair cells and marginal cells.

Increases doses of a constant molar ratio of GT:GTTR (300:1) resulted in increasing intensities of GTTR fluorescence in hair cells and stria tissues. This indicates that increased GTTR uptake in cochlear cells can be correlated to an increased GTTR dose as the total GT dose increases. Alternatively, the increased GT dose may induce cytotoxicity in the BLB, increasing the potential for GTTR to passively passage through a “leaky” BLB. Necrotic cells avidly bind GTTR, saturating the corresponding pixels during confocal acquisition (unpublished data), however, this was not observed within the stria vascularis in vivo in this acute study (3 hours). To address the possibility of a “leaky” barrier, two subsequent regimens were conducted.

Regimen 2: Constant GT dose, varying GTTR dose

Increasing molar dilution of GT:GTTR (150:1, 300:1 or 600:1) within a constant 300 mg/kg dose of GT produced decreasing intensities of GTTR fluorescence in hair cells and stria tissues. This regimen is useful because it confirmed that reducing the GTTR dose reduced GTTR fluorescence in all cochlear tissues, as observed in Regimen 1. However, the 600:1 molar dilution of GTTR in this regimen produced (qualitatively) less GTTR fluorescence in OHCs and marginal cells (Fig. 3C,F) compared to the same GTTR dose in Regimen 1 (150 mg/kg, 300:1 GT:GTTR; Fig. 1A,D). This suggested that competitive inhibition may also reduce uptake. Thus, to determine whether GTTR uptake is competitively inhibited by GT in cochlear tissues, we administered a constant GTTR dose, while increasing the GT dose and consequently the molar dilution of GTTR.

Regimen 3: Variable GT dose, constant GTTR dose

In Regimens 1 and 2, increasing the GTTR dose increased GTTR fluorescence in all cochlear tissues and capillaries, and in the relative density of fluorescent puncta in the immediate vicinity of the capillaries. In Regimen 3, stria capillaries did not show any significant difference in the intensity of GTTR fluorescence, even as the molar dilution increased, demonstrating that

GTTR access to the stria vascularis was not affected by changes in the GT dose. The (visible) density of fluorescent puncta in the immediate vicinity of the capillaries did not appear to differ significantly at any molar dilution, further suggesting that GTTR levels in serum were constant, since endocytotic uptake of GTTR is non-specific (Myrdal et al., 2005). Furthermore, the intra-stria tissues between the stria capillaries did not show any significant change in GTTR fluorescence as the molar dilution increased. In toto, this suggests that GTTR fluorescence in the intra-stria tissues is not saturable.

In contrast, increased levels of GT co-administered with a constant dose of GTTR (150:1–600:1 ratios) decreased GTTR uptake in hair cells and marginal cells *in vivo*, characteristic of competitive inhibition, and similar to *in vitro* data (Myrdal et al., 2005). *In vivo* inhibition of GTTR uptake was also observed in the cytoplasm of proximal tubule cells (Fig. 5), even as the density of fluorescent puncta in stria capillaries and proximal tubule cells appeared unchanged. Interestingly, no fluorescent puncta were readily observed in focal planes through marginal cells.

At very high molar dilutions (e.g., 900mg/kg, 900:1 GT:GTTR), GTTR fluorescence in hair cells and marginal cells was brighter than at 600mg/kg GT dose (600:1 GT:GTTR). This possibly indicates some form of dysfunction in the BLB facilitating GTTR entry into marginal cells, cochlear fluids and hair cells, since necrotic cells were not observed. Only 2 animals survived these high GT doses for 3 hours, and such doses are generally lethal to mice (Wu et al., 2001).

In other studies, the presence of mannitol (a probe of paracellular transport across epithelial and endothelial barriers) in perilymph or endolymph is not enhanced by pretreatment with GT levels that induce hair cell loss (Laurell et al., 2000). Thus, if paracellular routes across the BLB into the cochlear fluids are sealed, even during drug treatment, then GTTR most likely enters the cochlear fluids by transcellular routes in order to be taken up by hair cells.

Implications

In intra-stria tissues and capillaries, GTTR fluorescence appeared to correlate with GTTR dose, independently of the GT dose given. This suggests that intra-stria localization of GTTR is not saturable (or competitively inhibited). This could represent one or more mechanisms. Firstly, passive extravasation of GTTR from stria capillaries would not be competitively inhibited by GT (unless there is subsequent competition for GT binding prior to fixation). This could be tested by co-treatment with serotonin, or by electrical stimulation of the trigeminal ganglion, known enhancers of extravasation (Koo and Balaban, 2006; Vass et al., 2001). Membrane-compromised necrotic cells were not observed (due to lack of avidly GTTR-labeled cells).

Non-specific transcytosis may be one non-specific, rate-limiting mechanism that transfers GTTR into the intra-stria tissues that were less fluorescent than the stria capillaries. Capillary-associated fluorescent puncta were more readily visible as the GTTR dose increased in Regimens 1 and 2. However, at different molar ratios of GTTR in Regimen 3, little difference in density of capillary-associated fluorescent puncta could be observed, suggesting that endocytotic uptake of GTTR in the vicinity of the capillary wall is non-specific, as in the kidney (Fig. 5) and *in vitro* (Myrdal et al., 2005). In the spiral ligament and lateral wall, fluorescent puncta were present at lower densities than in stria tissues, similar to the findings of Sakagami et al. (1982). However, direct quantitation of transcytosis could not be made, as it was difficult to determine the density of fluorescent puncta due their wide variation in size, location in the stria vessel and tissues, intensity and frequency in the same specimen. Fluorescent puncta were not visible within the intra-stria tissues away from the capillaries, nor in marginal cells, suggesting that trans-stria transport requires other mechanisms besides transcytosis.

Alternatively, if aminoglycosides directly enter the cytoplasm of stria endothelial cells in a non-saturable manner, gap junctions could allow easy access to interconnected cellular compartments, specifically intermediate cells and basal cells (Takeuchi and Ando, 1998; Takeuchi et al., 2001).

In contrast to the non-saturable intra-stria tissues, GTTR fluorescence in marginal cells, OHCs and proximal tubule cells was competitively inhibited *in vivo* by increasing concentrations of GT. This corresponds to the *in vitro* data of Myrdal et al. (2005), where increasing GT concentrations reduced cytoplasmic uptake of GTTR in both proximal and distal tubule cell lines, and suggests that non-endocytotic transport mechanism(s) that enable(s) GTTR to enter marginal cells and proximal tubule cells *in vivo*. In further congruence with Myrdal et al. (2005), increasing GT concentrations did not inhibit or quench endosomal uptake of GTTR in proximal tubule cells *in vivo*, suggesting that non-endocytotic mechanisms are involved that can be competitively inhibited by GT to reduce cytoplasmic GTTR uptake by hair cells or marginal cells. Indeed, fluorescent puncta were not readily observed in marginal cells.

Competitive inhibition could occur at the pore/binding sites of aminoglycoside-permissive cation channels that facilitate GTTR entry into cells (Marcotti et al., 2005; Myrdal et al., 2005). More speculatively, competitive inhibition could also occur at transport protein binding sites. Both cation channels and ion transport proteins are prominently localized at the intra-stria face of both marginal cells and intermediate cells, presumably at densities that regulate can GTTR uptake. This potential regulatable barrier for GT is reminiscent of the intra-stria electrical boundary for potassium (Marcus et al., 2002; Wangemann, 2006).

Marginal cells lie in the endolymphatic domain, with an outward cationic current into endolymph (Lang et al., 2007; Wangemann, 2002). This suggests that marginal cells could potentially clear aminoglycosides into endolymph, from where these drugs could electrophoretically enter hair cells. Competitive inhibition of GTTR uptake by marginal cells would also be reflected in reduced clearance of GTTR into endolymph, and therefore reduced uptake of GTTR by hair cells, as observed. Indeed, there may be further competitive antagonism between GT and GTTR at the point of entry into hair cells through aminoglycoside-permissive channels, such as the mechanotransduction channel (Marcotti et al., 2005), as demonstrated by Gale et al. (2001). It is also likely that GT and GTTR have different rates of entry into cochlear tissues/fluids due to the smaller molecular weight of GT (449–477) compared to GTTR (approx. 1000–1100), although their pharmacokinetics are not addressed in this study.

Our data suggest that: (i) GTTR can enter the cochlea and stria tissues non-specifically, (ii) marginal cell uptake of GTTR can be competitively inhibited by native unconjugated gentamicin, demonstrating the bio-activity of GTTR; and (iii) GTTR (and thus GT) transport across the stria vascularis is regulatable at the marginal cell-intermediate cell boundary. If this regulatable mechanism is confirmed, this suggests two hypotheses for the observed inter-species differences for hair cell uptake of aminoglycosides. First, that the regulatable mechanism of aminoglycoside entry into murine marginal cells is unique, providing enhanced protection of marginal cells, endolymph and hair cells from noxious levels of aminoglycoside uptake and subsequent auditory dysfunction. Or secondly, that the regulatable mechanism of aminoglycoside uptake into murine marginal cells is inefficient (compared to guinea pigs and humans), inadvertently providing a barrier to aminoglycoside entry into marginal cells, and hence endolymph and hair cells. Conversely, guinea pigs and humans would need to possess an extremely efficient mechanism capable of transporting aminoglycosides against the electrical gradient, at the interface between marginal and intermediate cells. We are working to differentiate between these possibilities, and characterizing the various potential mechanisms for the trans-stria transport of gentamicin.

Acknowledgments

The authors thank Dennis Trune for insightful discussions on the manuscript, and Qi Wang for her assistance with image analysis. Funded by DC 04555 (PSS), and P30 DC 05983 grants from the National Institute of Communication and other Disorders, NIH; China Scholarship Council (No. 20361037) and the Educational Ministry of China grant NCET 06-0369 (CFD).

Abbreviations

BLB	blood-labyrinth barrier
GT	gentamicin
GTTR	gentamicin-Texas Red
hTR	hydrolyzed Texas Red
OHCs	outer hair cells
PBS	phosphate buffered saline

LITERATURE CITED

- Aran JM, Dulon D, Hiel H, Erre JP, Arousseau C. [Ototoxicity of aminosides: recent results on uptake and clearance of gentamycin by sensory cells of the cochlea]. *Rev Laryngol Otol Rhinol (Bord)* 1993;114:125–8. [PubMed: 8284554]
- Aran JM, Erre JP, Lima da Costa D, Debarh I, Dulon D. Acute and chronic effects of aminoglycosides on cochlear hair cells. *Ann N Y Acad Sci* 1999;884:60–8. [PubMed: 10842584]
- Bernard PA. Freedom from ototoxicity in aminoglycoside treated neonates: a mistaken notion. *Laryngoscope* 1981;91:1985–94. [PubMed: 7321720]
- Brummett RE. Effects of antibiotic-diuretic interactions in the guinea pig model of ototoxicity. *Reviews of infectious diseases* 1981;3(suppl):S216–23. [PubMed: 7342284]
- Dai CF, Mangiardi D, Cotanche DA, Steyger PS. Uptake of fluorescent gentamicin by vertebrate sensory cells in vivo. *Hear Res* 2006;213:64–78. [PubMed: 16466873]
- Dehne N, Rauen U, de Groot H, Lautermann J. Involvement of the mitochondrial permeability transition in gentamicin ototoxicity. *Hear Res* 2002;169:47–55. [PubMed: 12121739]
- Dulon D, Aran JM, Zajic G, Schacht J. Comparative uptake of gentamicin, netilmicin, and amikacin in the guinea pig cochlea and vestibule. *Antimicrob Agents Chemother* 1986;30:96–100. [PubMed: 3489440]
- Dulon D, Zajic G, Aran JM, Schacht J. Aminoglycoside antibiotics impair calcium entry but not viability and motility in isolated cochlear outer hair cells. *J Neurosci Res* 1989;24:338–46. [PubMed: 2585554]
- Dulon D, Hiel H, Arousseau C, Erre JP, Aran JM. Pharmacokinetics of gentamicin in the sensory hair cells of the organ of Corti: rapid uptake and long term persistence. *C R Acad Sci III* 1993;316:682–7. [PubMed: 8019890]
- Ehret G. Development of absolute auditory thresholds in the house mouse (*Mus musculus*). *J Am Audiol Soc* 1976;1:179–84. [PubMed: 956003]
- Gale JE, Marcotti W, Kennedy HJ, Kros CJ, Richardson GP. FM1–43 dye behaves as a permeant blocker of the hair-cell mechanotransducer channel. *J Neurosci* 2001;21:7013–25. [PubMed: 11549711]

- Harris JA, Cheng AG, Cunningham LL, MacDonald G, Raible DW, Rubel EW. Neomycin-induced hair cell death and rapid regeneration in the lateral line of zebrafish (*Danio rerio*). *J Assoc Res Otolaryngol* 2003;4:219–34. [PubMed: 12943374]
- Hashino E, Shero M. Endocytosis of aminoglycoside antibiotics in sensory hair cells. *Brain Res* 1995;704:135–40. [PubMed: 8750975]
- Hayashida T, Hiel H, Dulon D, Erre JP, Guilhaume A, Aran JM. Dynamic changes following combined treatment with gentamicin and ethacrynic acid with and without acoustic stimulation. Cellular uptake and functional correlates. *Acta Otolaryngol (Stockh)* 1989;108:404–13. [PubMed: 2589069]
- Henry KR, Chole RA, McGinn MD, Frush DP. Increased ototoxicity in both young and old mice. *Arch Otolaryngol* 1981;107:92–5. [PubMed: 7469897]
- Hiel H, Bennani H, Erre JP, Arousseau C, Aran JM. Kinetics of gentamicin in cochlear hair cells after chronic treatment. *Acta Otolaryngol* 1992;112:272–7. [PubMed: 1604991]
- Juhn SK, Hunter BA, Odland RM. Blood-labyrinth barrier and fluid dynamics of the inner ear. *Int Tinnitus J* 2001;7:72–83. [PubMed: 14689642]
- Koo JW, Balaban CD. Serotonin-induced plasma extravasation in the murine inner ear: possible mechanism of migraine-associated inner ear dysfunction. *Cephalalgia* 2006;26:1310–9. [PubMed: 17059438]
- Lang F, Vallon V, Knipper M, Wangemann P. Functional significance of channels and transporters expressed in the inner ear and kidney. *Am J Physiol Cell Physiol* 2007;293:C1187–208. [PubMed: 17670895]
- Laurell G, Viberg A, Teixeira M, Sterkers O, Ferrary E. Blood-perilymph barrier and ototoxicity: an in vivo study in the rat. *Acta Otolaryngol* 2000;120:796–803. [PubMed: 11132710]
- Lenoir M, Marot M, Uziel A. Comparative ototoxicity of four aminoglycosidic antibiotics during the critical period of cochlear development in the rat. A functional and structural study. *Acta Otolaryngol Suppl* 1983;405:1–16. [PubMed: 6586053]
- Marcotti W, van Netten SM, Kros CJ. The aminoglycoside antibiotic dihydrostreptomycin rapidly enters mouse outer hair cells through the mechano-electrical transducer channels. *J Physiol* 2005;567:505–21. [PubMed: 15994187]
- Marcus DC, Wu T, Wangemann P, Kofuji P. KCNJ10 (Kir4.1) potassium channel knockout abolishes endocochlear potential. *Am J Physiol Cell Physiol* 2002;282:C403–7. [PubMed: 11788352]
- Mathog RH, Capps MJ. Ototoxic interactions of ethacrynic acid and streptomycin. *Ann Otol Rhinol Laryngol* 1977;86:158–63. [PubMed: 300585]
- Meyers JR, MacDonald RB, Duggan A, Lenzi D, Standaert DG, Corwin JT, Corey DP. Lighting up the senses: FM1–43 loading of sensory cells through nonselective ion channels. *J Neurosci* 2003;23:4054–65. [PubMed: 12764092]
- Myrdal SE, Johnson KC, Steyger PS. Cytoplasmic and intra-nuclear binding of gentamicin does not require endocytosis. *Hear Res* 2005;204:156–69. [PubMed: 15925201]
- Owens KN, Cunningham DE, MacDonald G, Rubel EW, Raible DW, Pujol R. Ultrastructural analysis of aminoglycoside-induced hair cell death in the zebrafish lateral line reveals an early mitochondrial response. *J Comp Neurol* 2007;502:522–43. [PubMed: 17394157]
- Pujol R. Periods of sensitivity to antibiotic treatment. *Acta Otolaryngol Suppl* 1986;429:29–33. [PubMed: 3461671]
- Richardson GP, Russell IJ. Cochlear cultures as a model system for studying aminoglycoside induced ototoxicity. *Hear Res* 1991;53:293–311. [PubMed: 1880082]
- Rybak LP. Pathophysiology of furosemide ototoxicity. *J Otolaryngol* 1982;11:127–33. [PubMed: 7042998]
- Sakagami M, Matsunaga T, Hashimoto PH. Fine structure and permeability of capillaries in the stria vascularis and spiral ligament of the inner ear of the guinea pig. *Cell Tissue Res* 1982;226:511–22. [PubMed: 7139688]
- Sandoval R, Leiser J, Molitoris BA. Aminoglycoside antibiotics traffic to the Golgi complex in LLC-PK1 cells. *J Am Soc Nephrol* 1998;9:167–74. [PubMed: 9527392]
- Shnerson A, Pujol R. Age-related changes in the C57BL/6J mouse cochlea. I. Physiological findings. *Brain Res* 1981;254:65–75. [PubMed: 7272773]

- Steyger PS. Cellular uptake of aminoglycosides. *The Volta Review* 2005;105:299–324.
- Takeuchi S, Ando M. Dye-coupling of melanocytes with endothelial cells and pericytes in the cochlea of gerbils. *Cell Tissue Res* 1998;293:271–5. [PubMed: 9662649]
- Takeuchi S, Ando M, Sato T, Kakigi A. Three-dimensional and ultrastructural relationships between intermediate cells and capillaries in the gerbil stria vascularis. *Hear Res* 2001;155:103–12. [PubMed: 11335080]
- Ton C, Parnig C. The use of zebrafish for assessing ototoxic and otoprotective agents. *Hear Res* 2005;208:79–88. [PubMed: 16014323]
- Tran Ba Huy P, Bernard P, Schacht J. Kinetics of gentamicin uptake and release in the rat. Comparison of inner ear tissues and fluids with other organs. *J Clin Invest* 1986;77:1492–500. [PubMed: 3700652]
- Tran Ba Huy P, Manuel C, Meulemans A, Sterkers O, Wassef M, Amiel C. Ethacrynic acid facilitates gentamicin entry into endolymph of the rat. *Hear Res* 1983a;11:191–202. [PubMed: 6619004]
- Tran Ba Huy P, Meulemans A, Wassef M, Manuel C, Sterkers O, Amiel C. Gentamicin persistence in rat endolymph and perilymph after a two-day constant infusion. *Antimicrob Agents Chemother* 1983b;23:344–6. [PubMed: 6838193]
- Vass Z, Steyger PS, Hordichok AJ, Trune DR, Jancso G, Nuttall AL. Capsaicin stimulation of the cochlea and electric stimulation of the trigeminal ganglion mediate vascular permeability in cochlear and vertebro-basilar arteries: a potential cause of inner ear dysfunction in headache. *Neuroscience* 2001;103:189–201. [PubMed: 11311800]
- Wangemann P. K⁺ cycling and the endocochlear potential. *Hear Res* 2002;165:1–9. [PubMed: 12031509]
- Wangemann P. Supporting sensory transduction: cochlear fluid homeostasis and the endocochlear potential. *J Physiol* 2006;576:11–21. [PubMed: 16857713]
- Wu WJ, Sha SH, Schacht J. Recent advances in understanding aminoglycoside ototoxicity and its prevention. *Audiol Neurootol* 2002;7:171–4. [PubMed: 12053140]
- Wu WJ, Sha SH, McLaren JD, Kawamoto K, Raphael Y, Schacht J. Aminoglycoside ototoxicity in adult CBA, C57BL and BALB mice and the Sprague-Dawley rat. *Hear Res* 2001;158:165–78. [PubMed: 11506949]
- Yamane H, Nakai Y, Konishi K. Furosemide-induced alteration of drug pathway to cochlea. *Acta Otolaryngol Suppl* 1988;447:28–35. [PubMed: 3055805]

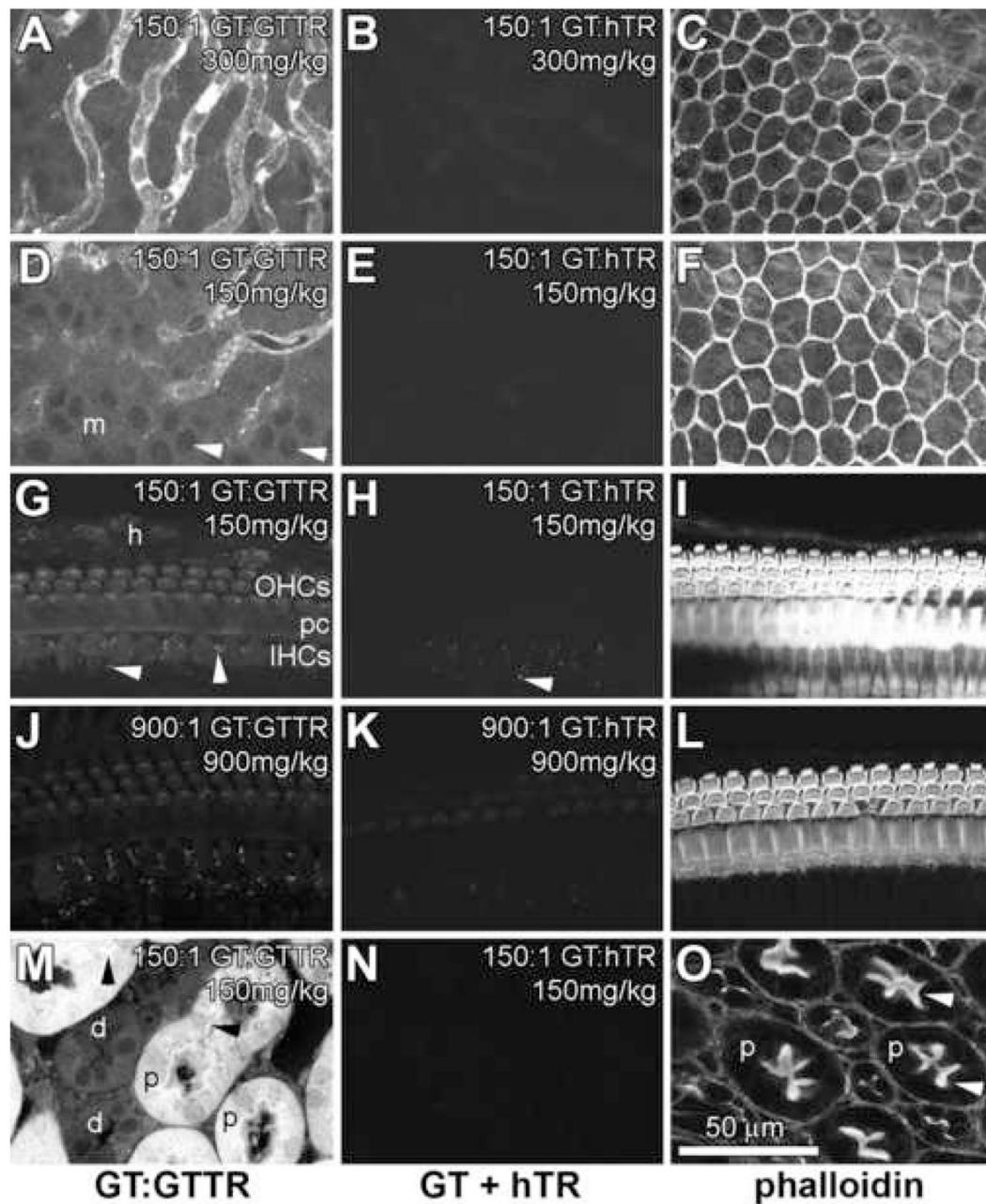


Figure 1. Distribution of GTTR and hTR fluorescence in cochlear (A–L) and kidney (M–O) tissues 3 hours after subcutaneous injection

(A) In the stria vascularis, punctate and diffuse GTTR fluorescence was most prominent in the tissues associated with the strial capillaries, with diffuse fluorescence in the intra-strial tissues between the capillaries. (B) In mice injected with hTR (and unconjugated GT, at the same dose as in A), negligible hTR fluorescence occurred in strial tissues. (C) Phalloidin-labeling of the image shown in B, showing the reticulated, actiniferous junctional complexes between adjacent marginal cells at the surface of the stria vascularis. (D) GTTR fluorescence in marginal cells (m) in this oblique focal plane, also showing punctate GTTR fluorescence in the region of the strial capillaries. Note the cytoplasmic labeling of GTTR delineating the nuclei of marginal cells (arrowheads). (E) In mice injected with hTR (and unconjugated GT at the same dose as

in D), negligible fluorescence occurred in marginal cells. (F) Phalloidin-labeling of the image shown in E. (G) In the organ of Corti, GTTR fluorescence was present in OHCs, IHCs, and pillar cells (pc), with less intense fluorescence in the Hensen's cells (h). Autofluorescent puncta (arrowheads) can be seen in supporting cells surrounding IHCs. (H) Autofluorescent puncta are also present in hTR-control tissues that display negligible hTR fluorescence in the organ of Corti. (I) Phalloidin-labeling of the image shown in H, showing the actiniferous structures of the organ of Corti. (J) High doses of GT decreased GTTR fluorescence in the organ of Corti (compare with G). (K) Negligible levels of hTR fluorescence in the organ of Corti of a mouse treated with a high dose of GT. (L) Phalloidin-labeling of the organ of Corti shown in K. (M) In vibrotome sections of the kidney, proximal tubule cells (p) contain both intense puncta (arrowheads) and diffuse cytoplasmic GTTR fluorescence. Distal tubule cells (d) exhibit less intense, diffuse cytoplasmic GTTR fluorescence. (N) Subcutaneous injection of hTR (with GT) revealed negligible hTR fluorescence in kidney tissues. (O) Phalloidin-labeling of the actiniferous brush borders (arrowheads) of proximal tubules shown in N. All GT + hTR images were acquired using the same laser intensity and confocal settings as tissues dosed with GT:GTTR. All cochlear images are from the mid-basal coil. Scale bar in microns.

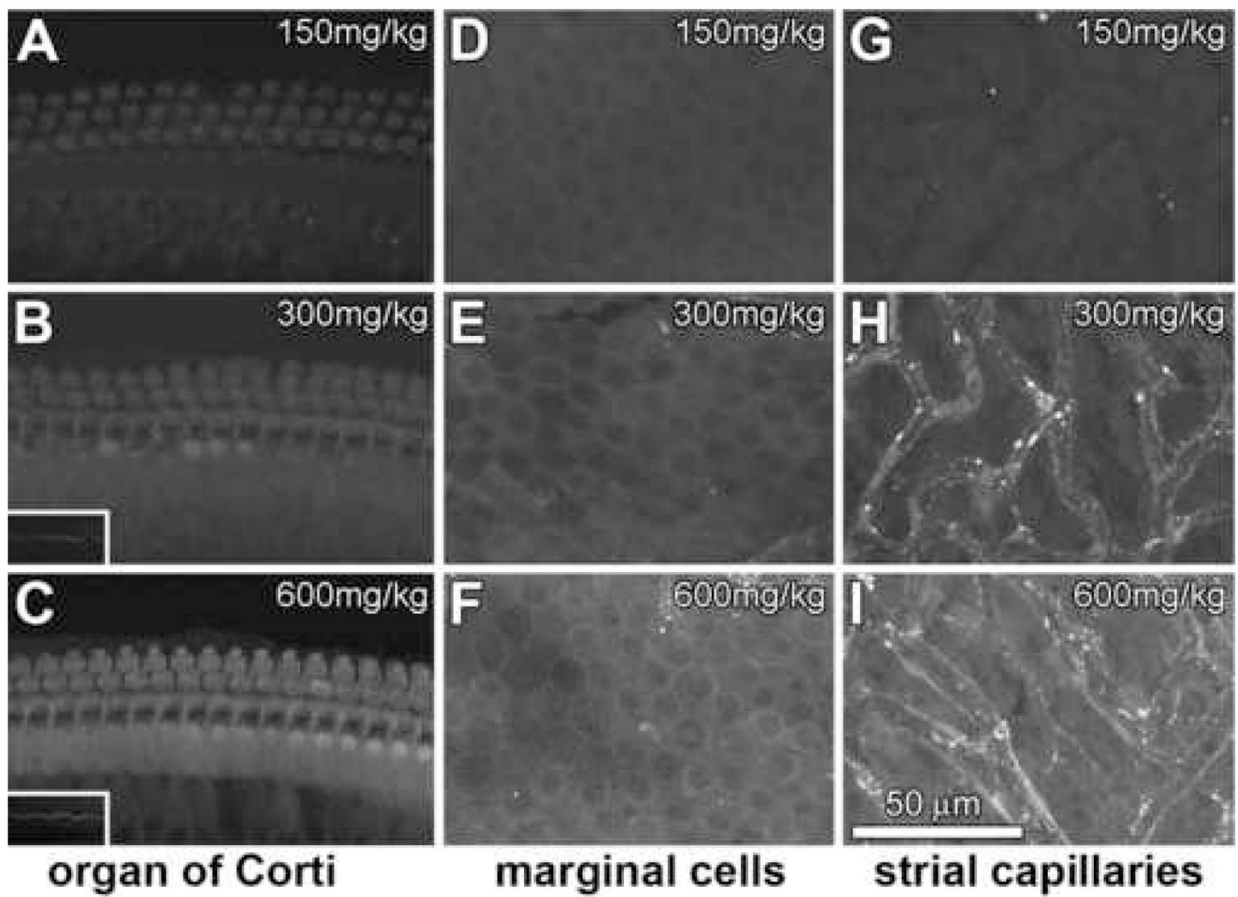


Figure 2. Constant GT:GTTR ratio. Mice received 150 (A,D,G), 300 (B,E,H), or 600 (C,F,I) mg/kg GT, each dose containing a 300:1 molar dilution of GT:GTTR

With increasing GT dose, increased intensities of GTTR fluorescence occur in hair cells (A–C), marginal cells (D–F) and intra-strial tissues (G–I). (A) Weak GTTR fluorescence in the cell bodies of IHCs, and pillar cells. (B) Increasing GTTR fluorescence in these same cells. IHC stereocilia are more readily observed (inset) at this higher dose. (C) At 600 mg/ml of 300:1 GT:GTTR, strong GTTR fluorescence can be seen in the organ of Corti, with distinct IHC stereociliary labeling (inset). (D–F) Marginal cells displayed increasing intensities of diffuse GTTR fluorescence with increasing dose. (Fluorescent puncta in E and F are from underlying capillaries, identified at immediately lower focal planes.) (G–I) Intra-strial tissues and capillaries also displayed increased intensities of GTTR fluorescence at higher GT doses, and fluorescent puncta in the immediate vicinity of capillaries. All images are from the mid-basal coil of the cochlea. All image sets acquired using the same laser intensity and confocal settings. Scale bar in microns.

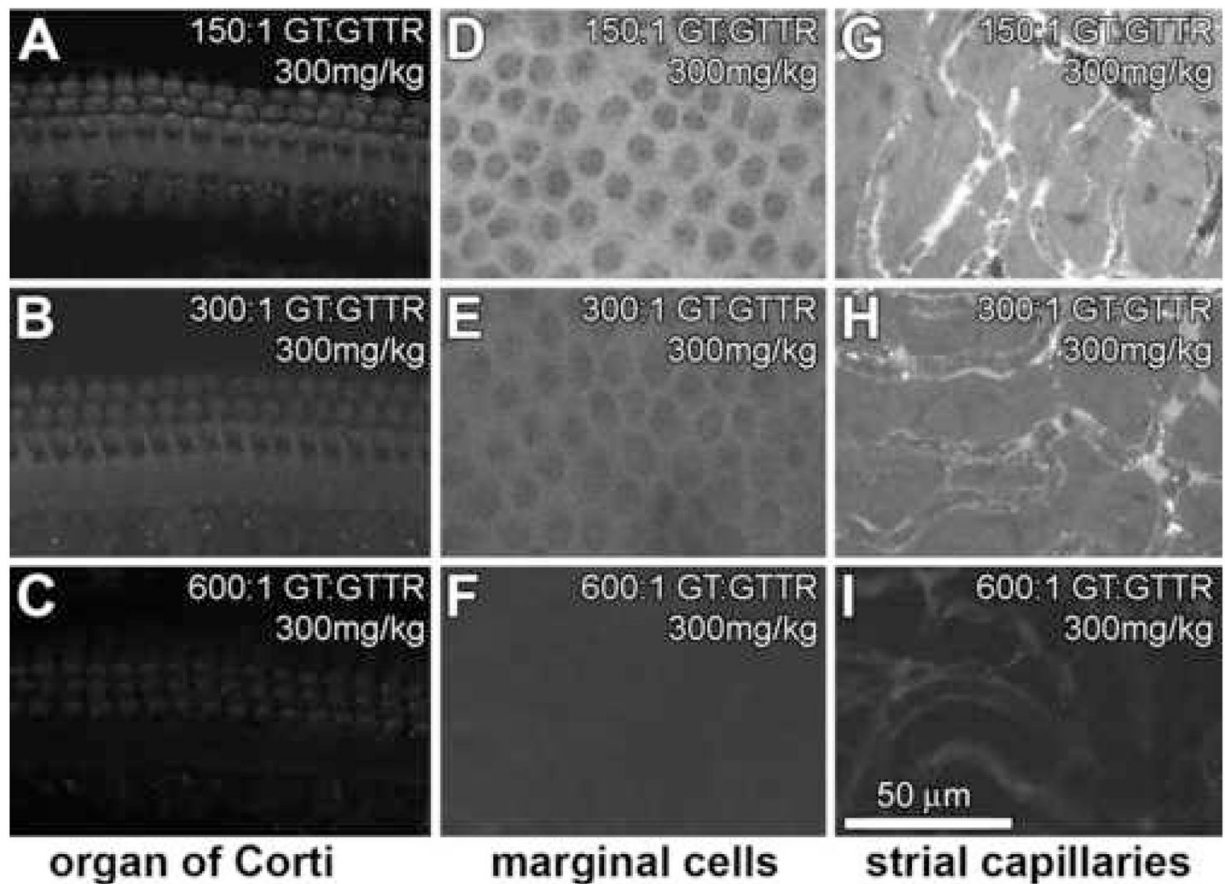


Figure 3. Constant GT dose, varying GTTR dose. Mice received a single injection of 300 mg/kg GT containing either 150:1 (A,D,G), 300:1 (B,E,H) or 600:1 (C,F,I) molar dilution of GT:GTTR. With increasing molar dilution of GTTR, decreasing intensities of GTTR fluorescence occur in hair cells (A–C), marginal cells (D–F) and tissues surrounding strial capillaries (G–I). Note the increased density of fluorescent puncta in G compared to I. All images are from the mid-basal coil of the cochlea. All image sets acquired using the same laser intensity and confocal settings. Scale bar in microns.

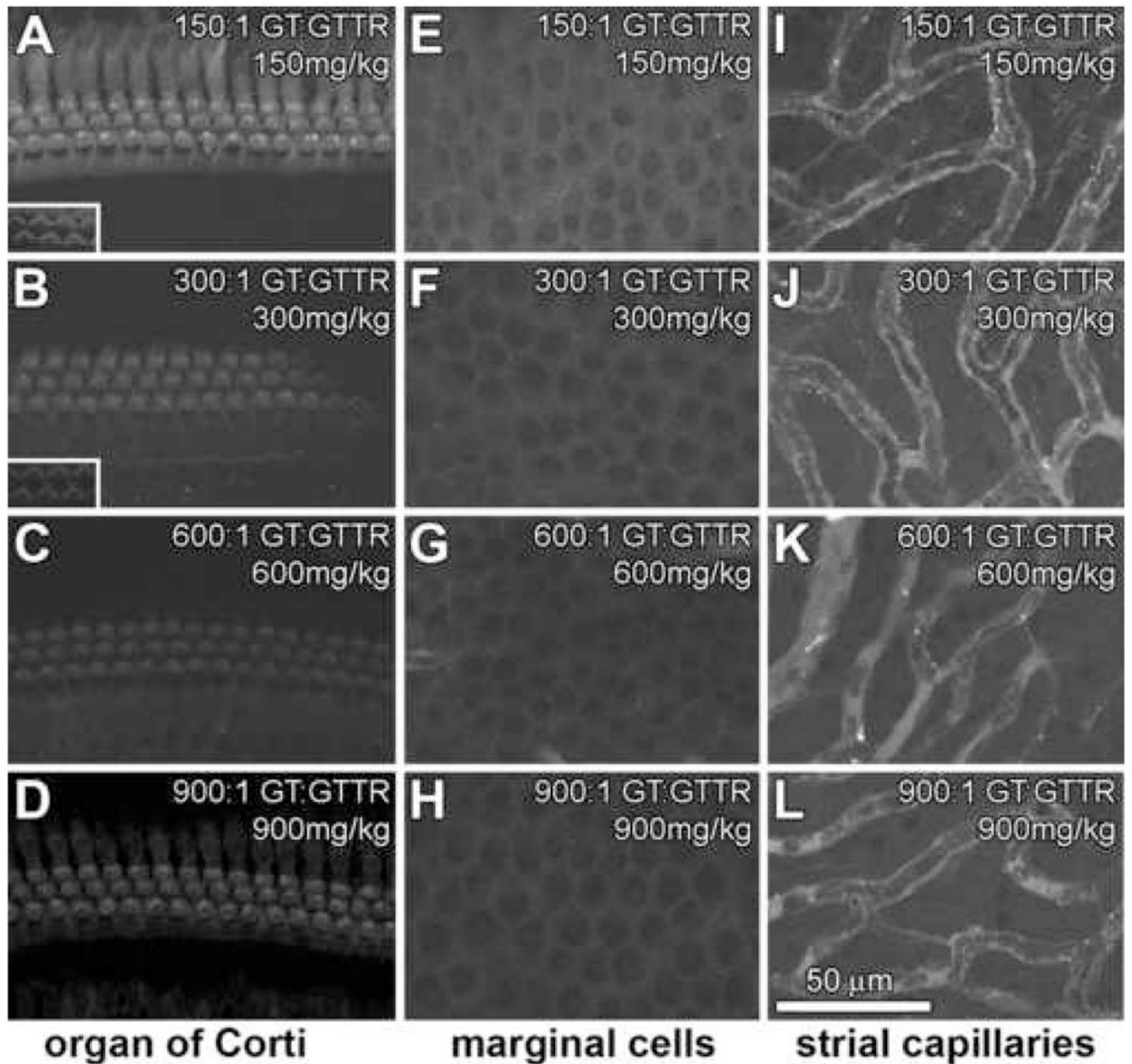


Figure 4. Variable GT dose, constant GTTR dose. Mice received equal amounts of GTTR (1.7 mg/kg) together with a GT dose of: 150 mg/kg (A,E,I), 300 mg/kg (B,F,J), 600 mg/kg (C,G,K) or 900 mg/kg (D,H,L)

With increasing molar dilution of GTTR, decreasing intensities of GTTR fluorescence occurred in hair cells (A–D) and marginal cells (E–F), but not in intr-strial tissues nor capillaries (I–L). In OHCs, treated with 900 mg/kg GT (900:1 GT:GTTR), GTTR fluorescence appeared more visibly intense in than at 600:1 GT:GTTR doses. Fluorescent puncta in the vicinity of strial capillaries are present at all molar dilutions (I–L). All images are from the mid-basal region of the cochlea. All image sets acquired using the same laser intensity and confocal settings. Scale bar in microns.

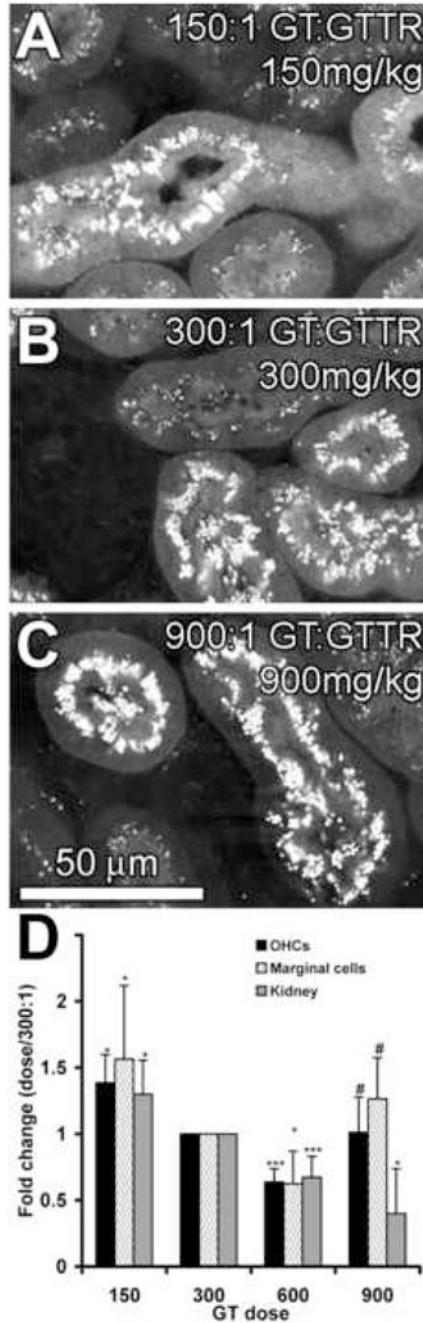


Figure 5. Variable GT dose, constant GTTR dose. Vibrotomed kidney sections from mice receiving equal amounts of GTTR (1.7 mg/kg) together with a GT dose of: 150 mg/kg (A), 300 mg/kg (B) or 900 mg/kg (C)

With increasing molar dilution of GTTR, decreasing intensities of GTTR fluorescence occurred in the cytoplasm of proximal tubule cells. Puncta of GTTR fluorescence did not appear to change with increasing GT dose. (D) Change in the intensity of GTTR fluorescence in OHCs, marginal cells and strial tissues, and proximal tubule cells as a function of GT dose in Regimen 3 (normalized against 300 mg/kg, 300:1 GT:GTTR dose); * = $p < 0.05$; *** = $p < 0.005$ against 300 mg/kg, 300:1 GT:GTTR dose; # = $p < 0.05$ against 600 mg/kg, 600:1 GT:GTTR dose.

Table 1

Tabulated guide to dosages. **Regimen 1:** a variable GT dose with a constant 300:1 molar ratio of GT:TR. **Regimen 2:** constant 300 mg/kg GT dose containing different molar ratios of GT:TR. **Regimen 3:** constant TR dose regardless of GT dose. Control mice received hydrolyzed Texas Red equivalent to the TR dose given above, in combination with unconjugated GT.

	Free GT (mg/kg)	Conjugated TR (mg/kg)	GT:TR molar ratio
Regimen 1			
	150	0.85	300:1
	300	1.7	300:1
	600	3.4	300:1
Regimen 2			
	300	3.4	150:1
	300	1.7	300:1
	300	0.85	600:1
Regimen 3			
	150	1.7	150:1
	300	1.7	300:1
	600	1.7	600:1
	900	1.7	900:1